Inelastic electron scattering from ^{29}Si

K. E. Whitner,* C. F. Williamson, B. E. Norum,† and S. Kowalski
Bates Linear Accelerator Center and Department of Physics, Massachusetts Institute of Technology, Cambridge, Massachusetts 02139
(Received 26 December 1979)

Electron scattering from ^{28}Si and ^{29}Si has been performed at energies from 126 to 293 MeV and at angles of 45° and 90°. Form factors were extracted for levels below 5.0 MeV in ^{28}Si and ^{29}Si over an effective momentum transfer range of 0.6 to 2.1 fm^{-1}. A particle-phonon coupling calculation using harmonic-oscillator single-particle states and data from ^{28}Si give a reasonable description of the low-lying states of ^{29}Si.

[NUCLEAR REACTIONS ^{28}Si(e,e') first 2 excited states; ^{29}Si(e,e') first 5 excited states; measured form factors 45° and 90°, $0.6 \leq q \leq 2.1$ fm^{-1}; natural Si target; PWBA analysis, vibrating core and intermediate coupling for ^{29}Si.]

I. INTRODUCTION

In 1950 Foldy and Milford[1] proposed an interaction between a valence particle and a liquid-drop nuclear core to explain the deviations of observed ground-state nuclear magnetic moments from the Schmidt limits. This interaction provided a mechanism for an exchange of angular momentum between the odd nucleon and the core[2] and explained qualitatively the direction of these deviations.

A more detailed development of the particle-surface coupling model was presented by Bohr[3] in 1952. Throughout the early 1950's, methods were developed for calculating nuclear energy levels, electromagnetic moments, and electromagnetic transition probabilities in weak, intermediate, and strong-coupling limits.[4-6] In general, strong-coupling limits were applied in the middle of major oscillator shells where nuclei are highly deformed, and weak or intermediate coupling limits were applied at or near closed shells.

During the next two decades many calculations were made for odd-mass nuclei. These calculations often successfully predicted the energies of the low-lying nuclear levels, but failed to explain adequately the static nuclear moments. Since few electromagnetic transition data existed at the time, it was difficult to test the calculations of transition strengths.

The ^{29}Si nucleus was one of the first isotopes to which the particle-core model was applied. Bohr and Mottelson[7] calculated the value of the ground-state magnetic moment in the strong-coupling limit. They showed that the Schmidt value, $-1.91\mu_N$, could be reduced to -1.0 to $-0.6\mu_N$, in closer agreement with the observed value of $-0.055\mu_N$. The suspected closure of the $1d_{5/2}$ shell at ^{28}Si, however, led some authors[8-10] to consider ^{29}Si in the intermediate-coupling approximation, in which the $2s_{1/2}$ and $1d_{3/2}$ single-particle orbitals were coupled to phonon states in ^{28}Si.

High-resolution electron scattering provides a very sensitive test for theoretical predictions of the structure of nuclear states. This experimental technique yields transition charge, current, and magnetization densities to these nuclear states as functions of momentum transfer. Corresponding transition densities can be calculated from the wave functions generated from a theoretical model. A comparison of the experimental and theoretical densities is a meaningful test of the theory because the interaction is relatively weak, and the electromagnetic transition operator is known.

Before approximately 1974 electron accelerator facilities could not provide the intense beam current and high ($\Delta p/p \sim 1 \times 10^{-4}$) resolution required to perform ^{29}Si or ^{30}Si scattering experiments with natural abundance silicon targets. Since natural silicon is 92.2% ^{28}Si, the energy levels of this isotope dominate the observed electron scattering spectrum of a natural silicon target. Thus, previous electron scattering measurements of the silicon isotopes were confined mainly to states in ^{28}Si.[11-16] The lone exception is the work of Brain *et al.*,[17] where a separated-isotope target of ^{29}Si was used in an electron scattering experiment which covered the momentum transfer range from 0.26 to 1.16 fm^{-1}.

The present paper presents experimental form factors for the ground state 0+, 1.78 MeV 2+, and 4.62 MeV 4+ levels in ^{28}Si and for four inelastic levels in ^{29}Si (1.27 MeV $\frac{3}{2}$+, 2.03 MeV $\frac{5}{2}$+, 2.43 MeV $\frac{3}{2}$+, and 4.08 MeV $\frac{7}{2}$+). The data cover a momentum transfer range from 0.6 to 2.1 fm^{-1}. Form factors for ^{30}Si and higher-

 © 1980 The American Physical Society

lying ^{29}Si and ^{28}Si states will be included in future work. Form factors for ^{29}Si calculated using an intermediate particle-phonon coupling scheme to combine ^{28}Si core states with single-particle states of the odd neutron are also presented. A comparison of theory to experiment shows good agreement for most of the levels studied.

II. EXPERIMENTAL METHODS

The present experiment was performed at the MIT-LNS Bates Linear Accelerator in Middleton, Massachusetts. The accelerator is described in detail in the literature.[18,19] Similarly, descriptions of the energy loss spectrometer system and focal plane instrumentation can be found in Refs. 20 and 21. The resolution $\Delta p/p$ ranged from 1.6×10^{-4} to 2.0×10^{-4}, and a typical electron scattering spectrum from natural Si is shown in Fig. 1. Average beam currents ranged from 4 to 40 μA, with 20–30 μA the most typical values.

Twenty-four measurements were made at different incident electron energies. Five of these runs were taken at a laboratory scattering angle of 45°, eighteen at 90°, and one was taken at 160°. The experimental parameters for these data runs are summarized in Table I. These energies and angles produced a range of effective momentum transfers, q_{eff}, of $0.6 \leq q_{eff} \leq 2.1$ fm^{-1} where

$$q_{eff} = q[1 + \tfrac{3}{2}(\tfrac{3}{5})^{1/2}(Z\alpha\hbar c/E_i R)].$$

Here Z is the atomic number, E_i is the bombarding energy, R is the rms nuclear radius, α is the fine-structure constant, and q is the kinematic momentum transfer.

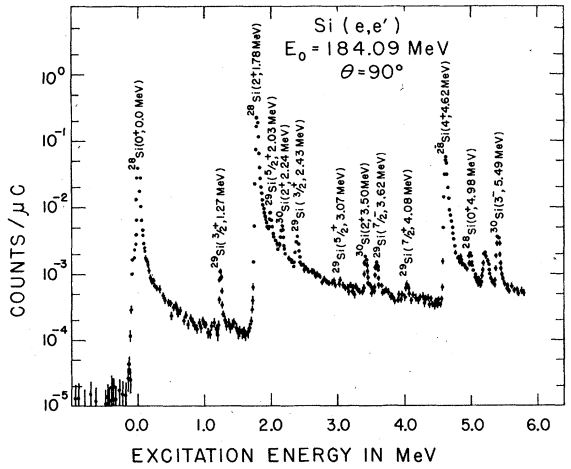

FIG. 1. Typical electron scattering spectrum from natural Si. This spectrum corresponds to Data Run No. 13 in Table I.

TABLE I. Summary of experimental conditions.

Data run	Incident[a] energy (MeV)	Angle[b] (deg)	Target thickness (mg/cm^2)
1	148.7	45.00	26.5±1.3
2	174.5	45.00	26.5±1.3
3	199.1	45.00	26.5±1.3
4	224.6	45.00	26.5±1.3
5	126.6	90.00	26.5±1.3
6	251.5	45.00	26.5±1.3
7	140.6	90.00	26.5±1.3
8	155.4	90.00	26.5±1.3
9	161.9	90.00	31.8±2.0
10	166.4	90.00	26.5±1.3
11	170.8	90.00	26.5±1.3
12	176.2	90.00	31.8±2.0
13	184.1	90.00	26.5±1.3
14	191.4	90.00	31.8±2.0
15	200.0	90.00	31.8±2.0
16	209.9	90.00	26.5±1.3
17	217.7	90.00	31.8±2.0
18	228.8	90.00	26.5±1.3
19	239.0	90.00	31.8±2.0
20	251.0	90.00	28.8±2.7
21	265.5	90.00	28.8±2.7
22	279.6	90.00	26.5±1.3
23	293.0	90.00	26.5±1.3
24	108.3	160.00	26.5±1.3

[a] The uncertainty in incident energy is ±0.3 MeV for all runs.

[b] The uncertainty in all angle measurements was ±0.05°.

A. Targets

The targets used in this experiment were cleaved natural silicon crystals; 92.2% ^{28}Si, 4.7% ^{29}Si, and 3.1% ^{30}Si. The targets were etched to their final thicknesses from 0.025 cm thick blanks using hydrofluoric, nitric, and acetic acids. No residual traces of these chemicals were observed in the targets.

The thickness of a standard silicon target was found in the following manner: At a fixed bombarding energy the scattering spectrum of the chosen target was compared with the scattering spectra of targets of other materials of known thicknesses to calculate a fit to the focal plane and accelerator energy parameters. Varying the silicon target thickness parameter in the calibration program resulted in a mapping of the fit chi square as a function of assumed target thickness. The target thickness corresponding to the minimum chi square was chosen as the correct value. An independent check was provided by a comparison of ^{28}Si data from this experiment with corresponding data from previous experiments. As can be seen in Fig. 2 the agreement with previous elastic scattering data is very good.

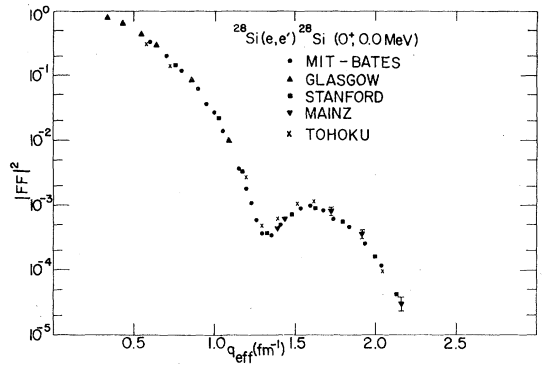

FIG. 2. Comparison of elastic scattering data for ^{28}Si from several different laboratories.

Thicknesses of the other three silicon targets were compared to the standard target by measuring the form factor of the ^{28}Si, 1.78 MeV 2^+ levels with all four targets.

Target uniformity was measured using attenuation of electrons emitted in the beta decay of ^{147}Pm following the procedure of Liljestrand *et al.*[22] A map of target thickness was made at a grid spacing of 1.25 mm by 2.5 mm. The average thickness in the beam spot area was found to vary by ±3%.

B. Data analysis

The raw spectra were corrected for count-rate losses and sorted into equal-width bins of nuclear excitation energy. Peak areas then were extracted from this corrected spectrum by use of a least-squares line-shape fitting routine. This code produced an eight-parameter semiempirical fit to each peak in the spectrum. In order to check the consistency of the fit, the integration of the peak area was cut off at five energies from 0.5 to 3.0 MeV above the excitation energy of the peak. A radiative correction was calculated for each cutoff energy and applied to the corresponding integrated peak area. A fit was judged acceptable if the five corrected peak areas agreed to within ±2.0%. The statistical errors in the peak area calculations were computed using an algorithm outlined by Bevington.[23] These errors are shown as error bars in the figures and as percent uncertainties in Tables VI and VII.

The experimental squared form factor $|F|^2$ was calculated from the peak area using

$$|F|^2 = \frac{\eta Z^2 Y e}{N_t \sigma_M (\Delta\Omega)} = \frac{\eta}{\sigma_M}\frac{d\sigma}{d\Omega},$$

where η is the nuclear recoil factor $[1+2E_i \sin^2(\theta/2)/M]$, σ_M is the Mott cross section $[Z\alpha\hbar c \cos(\theta/2)/2E_i \sin^2(\theta/2)]^2$, Z is the atomic number of target nucleus, M is the mass of target in MeV, E_i is the incident energy in MeV, Y is the corrected peak area in counts/unit charge, e is the electronic charge, $\Delta\Omega$ is the spectrometer solid angle acceptance, N_t is the number of nuclei in target/unit area, θ is the laboratory scattering angle, and $d\sigma/d\Omega$ is the differential scattering cross section. The form factors presented in this paper are all absolute measurements.

C. Systematic errors

The statistical errors are not the only contribution to experimental uncertainties. The main sources of systematic errors are summarized in Table II. Contributions from scattering-angle measurement, charge integration, detector inefficiency, and solid-angle measurement inaccuracies are not expected to vary for different runs. In principle, errors in energy calibration, count-rate corrections, and target parameters are more difficult to characterize and must be determined separately for each run. In the present work, however, the main limitation on experimental accuracy was the knowledge of the target thicknesses and uniformities. Other corrections varied little from run to run.

Since systematic errors in general do not obey simple statistical distribution laws, it is difficult to combine errors from different sources. Therefore, in the tables and figures only statistical errors are shown. An upper-limit estimate of the systematic errors for each data point is 7–10%.

III. THEORETICAL CALCULATIONS

The formalism of the particle-phonon coupling model has been extensively developed and can be found in the original papers by Bohr and Mottelson,[7] and Choudhury,[5] and in most texts on nuclear models.

A. Eigenvectors of ^{29}Si

The intermediate-coupling case considered here treats the particle-surface interaction operator

TABLE II. Principal sources of systematic errors.

Machine energy calibration	(±0.3 MeV)
Scattering angle	(±0.05 deg)
Charge integration	(±1.0%)
Solid angle	(±0.5%)
Overall detector inefficiency	(±2.0%)
Dead-time corrections $(1+f)$	(±20×f%)
Target thickness	(±5–10 %)
Target composition	(±1.0%)
Target uniformity	(±3.0%)
Radiative corrections	(±2.0%)

as a perturbation to the collective core motion plus the odd-neutron single-particle motion. The basis chosen to describe the ^{29}Si system is a linear combination of product states of ^{28}Si core states and s-d shell single-particle states. These are coupled to give the wave functions of the ^{29}Si levels. Numerical values for the energy levels and eigenvectors are obtained by fitting to known levels in ^{28}Si and ^{29}Si.[24]

These eigenvector calculations were chosen for comparison to the ^{29}Si data: the small basis (present work), the basis of Pandya,[8] and the basis of Castel *et al.*[10] The main differences are the number of single-particle and ^{28}Si core states included in the calculations. Tables III–V give the eigenvectors of the low-lying ^{29}Si levels obtained from the three calculations.

The theoretical spectra are compared to the actual ^{29}Si spectrum in Fig. 3. The small basis calculation uses as input the energies of the ground state and the $\frac{5}{2}$+ levels, thus predicting only the $\frac{3}{2}$+ and $\frac{7}{2}$+ energies. The inclusion in Ref. 8 of three two-phonon states (0+, 2+, 4+) at twice the energy of the one-phonon state in ^{28}Si, does not improve significantly the low-lying spectrum predictions over those of the small basis. The calculation of Ref. 10, however, reproduces very well the energies of the first four excited ^{29}Si levels.

B. ^{29}Si reduced matrix elements

The inelastic form factors for electron scattering for the low-lying ^{29}Si levels can be calculated from the reduced matrix elements (RME's) of the contributing electromagnetic multipole operators between ^{29}Si ground (initial) and ^{29}Si excited (final) states. Since each ^{29}Si state is a combination of product states describing the core and s-d shell single-particle contributions, the matrix element of the operator $O(\lambda, \mu)$ with angular momentum λ and projection μ will be a sum involving the components of the ^{29}Si eigenvectors. The electromagnetic interaction is sufficiently weak that $O(\lambda, \mu)$ can be written as a sum of A one-body operators, where A is the atomic mass number. In this calculation the sum over $A-1$ nucleons is the ^{29}Si core phonon operator, and the remaining operator is the single-particle operator. Since each operator acts on only one of the two components of each product state, the matrix element for the total operator breaks into a sum of matrix elements involving only phonon or only single-particle transitions.

Using the Wigner-Eckart theorem it is possible to define the RME of the operator $O(\lambda, \mu)$ from the matrix element

$$\langle JM \,|\, O(\lambda, \mu) \mathcal{J}\mathfrak{M}\rangle = (2J+1)^{-1/2}(-1)^{\lambda-\mathcal{J}+J} \times \langle \lambda\mu\mathcal{J}\mathfrak{M} \,|\, JM\rangle \langle J \,||\, O(\lambda) \,||\, \mathcal{J}\rangle .$$

This definition can be applied to both the total and constituent matrix elements to remove dependence on the particular angular-momentum projection. Thus the problem of finding an RME for a transition to an excited ^{29}Si state is reduced to a calculation of RME's for ^{28}Si phonon and s-d shell single-particle transitions.

C. Phonon reduced matrix elements

Phonon RME's (PHRME's) can be calculated in a straightforward manner using the liquid-drop multipole operator of Walecka[25] in terms of an equilibrium radius a and a scaling constant K which is proportional to the square of the phonon frequency. Since the ground state of ^{29}Si has $J^\pi = \frac{1}{2}^+$ and the excited states of interest have $J^\pi = \frac{7}{2}^+$, $\frac{5}{2}^+$, $\frac{3}{2}^+$, only $L=2$ and $L=4$ phonon transitions can contribute to the form factors of these states.

The RME's calculated according to the sharp-edged liquid-drop model of Ref. 25 were modified to include the effects of diffuseness of the nuclear surface through multiplication by a factor of $\exp(-G^2q^2/2)$.[26] In this formula G is a diffuseness parameter whose value is approximately equal to

TABLE III. Configuration of ^{29}Si states small basis.

	J	$\frac{1}{2}$	$\frac{3}{2}$	$\frac{5}{2}$	$\frac{3}{2}$	$\frac{5}{2}$	$\frac{7}{2}$
E_{exp}		0	1.27	2.03	2.43	3.07	4.08
E_{fit}		0	0.78	2.03	2.27	3.07	3.07
N L	j						
0 0	$\frac{1}{2}$	0.9617					
	$\frac{3}{2}$		0.8570		0.3420		
1 2	$\frac{1}{2}$		0.4239	1.000	−0.8779		
	$\frac{3}{2}$	−0.2742	−0.2930		−0.3353	1.000	1.000

TABLE IV. Configuration of ^{29}Si states basis of Ref. 8.

	J	$\frac{1}{2}$	$\frac{3}{2}$	$\frac{5}{2}$	$\frac{3}{2}$	$\frac{5}{2}$	$\frac{7}{2}$
E_{exp}		0	1.27	2.03	2.43	3.07	4.08
E_{fit}		0	0.80	1.68	2.43	3.03	
NL	j						
0 0	$\frac{1}{2}$	0.9200					
	$\frac{3}{2}$		0.7090		0.3400		
1 2	$\frac{1}{2}$		−0.6050	0.9190	0.6770	0.1290	
	$\frac{3}{2}$	0.3770	−0.2930	−0.0850	−0.5010	0.8230	
2 4	$\frac{1}{2}$						
	$\frac{3}{2}$			0.3550		−0.1650	
2 0	$\frac{1}{2}$	0.0810					
	$\frac{3}{2}$		0.1170		−0.0230		
2 2	$\frac{1}{2}$		0.1030	−0.0210	0.3380	0.4530	
	$\frac{3}{2}$	−0.0780	0.1470	0.1450	−0.2460	0.2720	

the proton rms radius. Form factors of the 2+ (1.78 MeV) and 4+ (4.61 MeV) levels in ^{28}Si were fitted to the experimental data using the functional forms

$$|F|^2 = \frac{4\pi K}{2J_i+1}\,[f_L(qa)]^2 \exp(-G^2q^2)\,,$$

$$f_2(qa) = j_2(qa)\,,$$

$$f_4(qa) = j_4(qa) - \tfrac{1}{6}\,qaj_5(qa)\,,$$

where $j_L(x)$ is the spherical Bessel function of order L. The frequency parameter K and the radius parameter a were allowed to vary to obtain the best fit. The diffuseness parameter G^2 was fixed at 0.693 fm^2. The PHRME is then given by

$$\langle NL\,||O(\lambda)||\,00\rangle = K^{1/2} f_L(qa)\exp(-G^2q^2/2)\,.$$

The fits to the ^{28}Si data are shown in Fig. 3 for the 2+ and 4+ transitions. Transitions to the 0+ (4.98 MeV) state cannot contribute to the inelastic

TABLE V. Configuration of ^{29}Si states basis of Ref. 10.

		J	$\frac{1}{2}$	$\frac{3}{2}$	$\frac{5}{2}$	$\frac{3}{2}$	$\frac{5}{2}$	$\frac{7}{2}$
E_{exp}			0	1.27	2.03	2.43	3.07	4.08
E_{fit}			0	1.27	2.01	2.46	3.18	3.43
N	L	j						
0	0	$\frac{1}{2}$	0.9753					
		$\frac{3}{2}$		0.8942		0.3904		
		$\frac{5}{2}$			−0.3493		0.7923	
1	2	$\frac{1}{2}$		−0.4055	0.9244	0.9088	0.3157	
		$\frac{3}{2}$	0.1669	−0.1724	0.0317	−0.1199	−0.4765	0.9552
		$\frac{5}{2}$	0.1404	0.0662	0.0366	0.0329	−0.1811	0.0303
2	4	$\frac{1}{2}$						−0.2580
		$\frac{3}{2}$			0.1238		0.1059	−0.1359
		$\frac{5}{2}$		−0.0336	0.0705	0.0655	−0.0089	0.0405
2	0	$\frac{1}{2}$	−0.0336					
		$\frac{3}{2}$		0.0282		−0.0431		
		$\frac{5}{2}$			0.0342		0.0362	

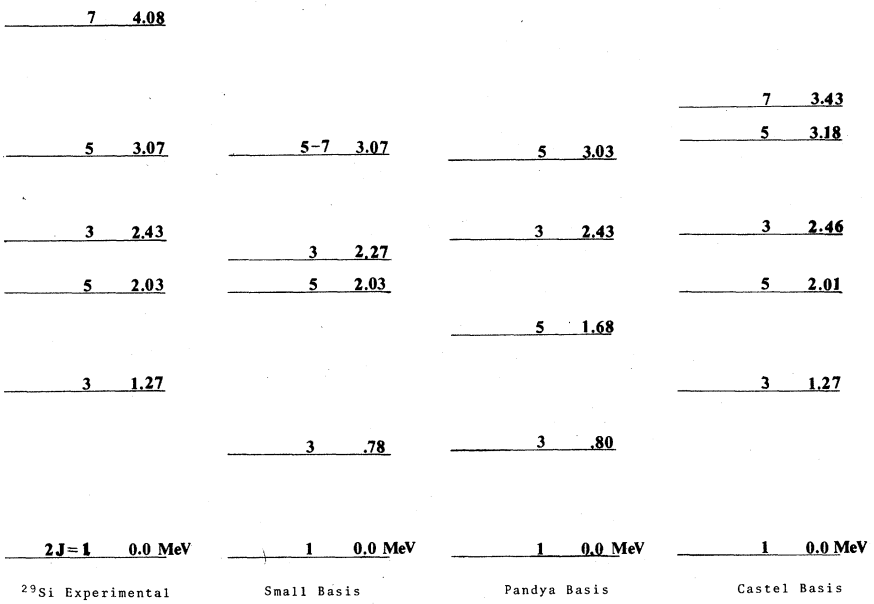

FIG. 3. Energy levels in ^{29}Si as predicted using three sets of basis vectors compared to the experimental level diagram.

form factors calculated here. The two-phonon 2+ used in Ref. 8 has not been included as this level does not exist below 5.0 MeV in the ^{28}Si spectrum.

One assumption implicit in the above discussion is that the transverse form factors F_T^2 of the ^{28}Si 2+ and 4+ states are negligible. This assumption was checked by comparing data at the same q_{eff}, but at 160° and 90° to find the value of the transverse form factor. For both the 2+ (1.78 MeV) and 4+ (4.61 MeV) levels the contribution at 90° from transverse scattering was found to be less than 4%. Thus the assumption of a negligible contribution from the transverse form factor is valid at the scattering angles used in this experiment.

Some of the PHRME's required in the calculation represent transitions between excited states in the ^{28}Si core. The functional form of these PHRME's was calculated using the diffuse-edge, liquid-drop model. The radius and scaling parameters were obtained from the fits to the ^{28}Si experimental form factors of the corresponding multipolarity.

D. Single-particle reduced matrix elements

Single-particle reduced matrix elements (SPRME's) were calculated using harmonic-oscillator wave functions and the formalism of Willey.[27] The oscillator parameter for the $1d_{5/2}$ shell was taken from Müllhaupt[13] to be $d=1.88$ fm. The neutron parameters used here were an effective charge of $0.5e$, and a magnetic moment of $-1.91\,\mu_N$. Both center-of-mass and finite nucleon size corrections were made to the resulting RME's.[27,28]

E. Calculation of ^{29}Si form factors

The squared form factors for ^{29}Si states were calculated using the formalism described in the previous sections according to

$$|F|^2=\frac{4\pi\epsilon^2}{Z^2}\,\frac{1}{2J_i+1}\sum_\lambda\{|\langle f||O_L(\lambda)||i\rangle_t|^2 + (\tfrac{1}{2}+\tan^2\theta/2)\times[|\langle f||O_E(\lambda)||i\rangle_t|^2 + |\langle f||O_M(\lambda)||i\rangle_t|^2]\}.$$

In this formula J_i is the spin of the initial state; λ is the multipolarity of the transition; $|i\rangle$ and $|f\rangle$ are, respectively, the eigenvectors of the initial and final states; the subscripts L, E, and M refer, respectively, to the longitudinal, transverse electric, and transverse magnetic transitions; and ϵ is the effective charge of the valence neutron. (In the present calculation, ϵ was taken to be 0.5.) The subscript t indicates that these are total reduced matrix elements for the transition. The total reduced matrix elements are sums of PHRME's and SPRME's. The summation on λ is extended over all allowed transition multipolarities.

IV. RESULTS AND DISCUSSION

The experimental form factors are given for ^{28}Si in Table VI and for ^{29}Si in Table VII. These

TABLE VI. Electron scattering squared form factors for levels in ^{28}Si. [a,b]

	0^+ (0.00 MeV)			2^+ (1.78 MeV)			4^+ (4.62 MeV)		
Run	q_{eff} (fm^{-1})	$\|F\|^2$ $\times 10^{-4}$	± %	q_{eff} (fm^{-1})	$\|F\|^2$ $\times 10^{-5}$	± %	q_{eff} (fm^{-1})	$\|F\|^2$ $\times 10^{-5}$	± %
1	0.601	3270	0.72	0.597	443	0.72			
2	0.701	2000	0.67	0.698	617	0.94	0.692	4.10	21
3	0.796	1150	0.54	0.793	658	1.64	0.787	7.31	7.1
4	0.895	613	0.74	0.891	691	1.14	0.886	15.2	4.2
5	0.951	361	0.97	0.944	626	0.70	0.934	16.2	3.0
6	0.999	261	0.88	0.995	636	0.81	0.990	24.9	7.9
7	1.051	138	0.64	1.044	561	0.61	1.034	27.4	2.4
8	1.156	36.5	2.0	1.149	425	0.65	1.139	36.5	2.5
9	1.203	17.6	0.81	1.196	337	0.47	1.186	37.7	1.06
10	1.234	10.6	0.51	1.228	324	0.55	1.217	42.6	1.28
11	1.266	5.89	3.87	1.259	271	0.37	1.250	44.7	0.54
12	1.304	3.62	8.31	1.297	243	0.55	1.287	49.2	2.5
13	1.360	3.32	1.15	1.354	159	0.45	1.340	47.9	0.82
14	1.412	4.89	3.1	1.406	126	0.89	1.396	50.9	1.38
15				1.467	63.3	0.86	1.458	49.6	1.35
16	1.544	8.77	0.42	1.537	32.4	1.17	1.530	45.6	1.27
17	1.599	9.60	1.12	1.593	17.7	2.5	1.580	44.6	3.3
18	1.678	8.22	0.54	1.672	3.62	2.1	1.660	35.9	1.68
19	1.744	6.08	0.73	1.737	0.932	6.7	1.734	26.9	2.9
20	1.836	4.60	0.95	1.830	3.35	3.9	1.819	23.4	1.53
21	1.939	2.49	1.13	1.932	7.81	2.7	1.922	15.3	1.85
22	2.039	1.12	1.88	2.032	10.5	1.09	2.020	8.81	1.43
23	2.134	0.417	1.68	2.127	10.9	1.01	2.120	4.98	6.4
24				1.131	397	3.5			

[a] The squared form factor should be multiplied by the indicated factor.
[b] Percentage errors are statistical only.

data are also presented in graphical form in Figs. 4(a) and 4(b) and 5(a)–5(e).

The data on the ^{28}Si ground state from this experiment agree with most of the previous measurements.[11-16] Discrepancies in the height of the second maximum result primarily from use of the Born approximation to extract the form factor, and the use of q_{eff} to compare data taken at different energies and angles. This agreement indicates that the experimental uncertainties in the absolute cross sections are small.

The liquid-drop parametrization used here adequately fits the form factors for the ^{28}Si 2+ and 4+ levels over most of the momentum transfer range of this experiment. Previous electron scattering measurements of Mülhaupt[13] and Nakada and Torizuka[14] have used both Helm[26] model and Nilsson[29] model fits to parametrize the data. Using the form factors of ^{28}Si to distinguish between the different descriptions of the core is difficult since the data can be parametrized by all three models. The choice of the vibrational model was a convenient one for this calculation, but the agreement between the calculations and the data should not be interpreted as evidence that ^{28}Si is a vibrational nucleus.

Results of the particle-phonon coupling calculation for the three bases of ^{29}Si are shown in Figs. 5(a)–5(e) along with the data. The calculations with the three bases work reasonably well for the 1.27 MeV $\frac{3}{2}$+, the 2.03 MeV $\frac{3}{2}$+, and the 2.43 MeV $\frac{3}{2}$+ levels. However, the prediction of Ref. 10 overestimates the actual form factor of the 3.07 MeV level. The single datum in Fig. 5(d) for the 3.07 MeV $\frac{5}{2}$+ level is shown to indicate the upper limit on the form factor of this state. None of the calculations adequately describes the 4.08 MeV $\frac{7}{2}$+ level.

The eigenfunctions depend on the choice of the basis vectors, the form of the system Hamiltonian, and the energy levels of ^{28}Si and ^{29}Si. All three eigenfunction calculations use the same form of the system Hamiltonian. The calculations with the small basis and the basis of Ref. 10 use the actual ^{28}Si energy levels while the calculation of Ref. 8 uses a true vibrational model for the ^{28}Si energies.

The basis of Ref. 8 is the least realistic, as indicated by the poor agreement of the calculation with the data. In this calculation all excited states include sizable contributions from the nonexistent two-phonon 2+ state. In addition, the 4+ and 0+

TABLE VII. Electron scattering squared form factors for levels in ^{29}Si. [a,b]

Run	$\frac{3}{2}^+$ (1.27 MeV) q_{eff} (fm^{-1})	$\|F\|^2$ ×10^{-5}	± %	$\frac{5}{2}^+$ (2.03 MeV) q_{eff} (fm^{-1})	$\|F\|^2$ ×10^{-5}	± %	$\frac{3}{2}^+$ (2.43 MeV) q_{eff} (fm^{-1})	$\|F\|^2$ ×10^{-5}	± %	$\frac{7}{2}^+$ (4.08 MeV) q_{eff} (fm^{-1})	$\|F\|^2$ ×10^{-5}	± %
1							0.596	113	38			
2	0.698	130	75	0.697	294	13	0.696	169	18.4			
3	0.794	129	55	0.792	331	8.8	0.791	147	15.1			
4	0.892	81.8	36	0.890	355	5.9	0.890	128	11.7			
5	0.946	84.7	21	0.943	304	5.8	0.942	136	9.1			
6	0.996	82.1	24	0.995	331	6.0	0.994	120	9.7			
7	1.046	64.8	13.3	1.044	252	5.9	1.041	124	7.2			
8	1.151	48.6	10.0	1.149	181	6.4	1.148	88.1	8.4			
9	1.198	37.3	10.3	1.195	137	5.2	1.193	73.0	6.2			
10	1.229	29.1	5.0	1.226	122	6.7	1.225	67.5	7.8	1.219	2.42	62
11	1.261	24.3	5.2	1.258	108	4.4	1.257	61.4	4.8	1.251	2.33	66
12	1.299	20.1	10.5	1.296	97.2	6.9	1.295	44.3	8.9			
13	1.356	13.0	5.6	1.352	64.2	5.3	1.351	37.5	5.7	1.346	4.05	25
14	1.408	8.63	25	1.405	46.9	10.3	1.403	28.9	10.5	1.397	6.29	25
15							1.464	15.5	10.8	1.458	5.89	16.5
16				1.536	10.7	12.5	1.535	7.60	11.5	1.530	5.51	10.2
17	1.595	0.96	121				1.590	1.88	61	1.584	7.07	14.8
18	1.673	0.28	179	1.670	1.10	49				1.663	5.07	9.9
19										1.736	5.32	12.9
20	1.831	1.72	49	1.829	2.98	18.7	1.827	1.94	36	1.821	4.95	15.5
21				1.931	3.36	41				1.923	3.48	15.8
22	2.034	2.11	11.0	2.031	4.39	15.8	2.029	2.41	17.2	2.024	3.00	11.6
23	2.129	2.63	10.6	2.126	4.86	17.5	2.125	2.68	16.3	2.119	2.18	14.1
24												

[a] The squared form factor entries should be multiplied by the indicated factor.
[b] Percentage errors are statistical only.

levels are assumed to be at twice the energy of the one-phonon level instead of the actual ^{28}Si level energies.

The description of the ^{28}Si core in Ref. 10 offers an improvement on the predictions of Ref. 8. The Ref. 10 basis also describes the shape and scaling of the 2.43 MeV $\frac{3}{2}$+ level and the shape of the 1.27 MeV $\frac{3}{2}$+ level better than the small basis calculation. The Ref. 10 basis, however, overestimates by an order of magnitude the stregnth of the 3.07 MeV $\frac{5}{2}$+ level and overestimates slightly the strength of the 2.03 MeV $\frac{5}{2}$+ level. The chief problem seems to be the inclusion of the $1d_{5/2}$ single-particle state in the configurations. In this calculation the $1d_{5/2}$ coupled to the ground state 0+ is the main component of the 3.07 MeV level and is a substantial component of the 2.03 MeV level. It should be noted, however, that the calculations for those levels in Ref. 10 that contain very little $1d_{5/2}$ strength show good agreement with the data.

The PHRME's for ^{28}Si appearing in the calculation include both transitions from the ground

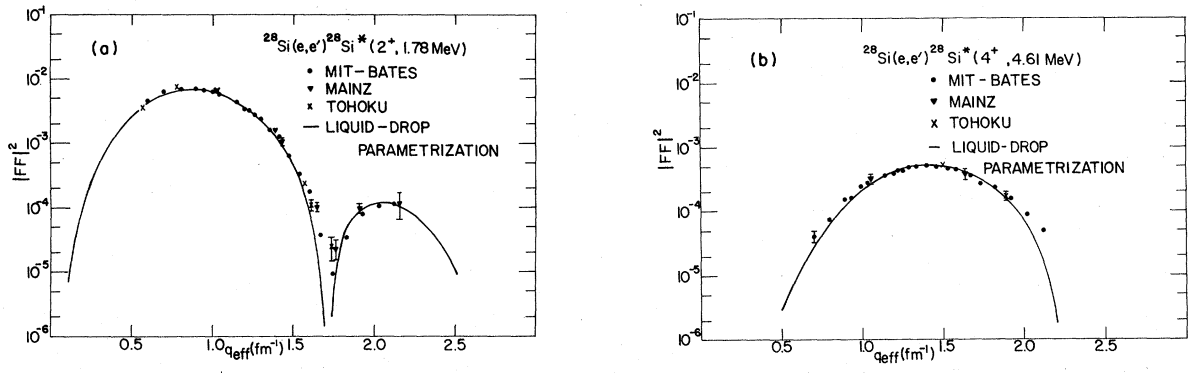

FIG. 4. Squared form factors for electron scattering from ^{28}Si. (a) 2$^+$(1.78 MeV) level. (b) 4$^+$(4.61 MeV) level. Data from three different laboratories are shown along with the fits to the diffuse edge vibrating liquid-drop model.

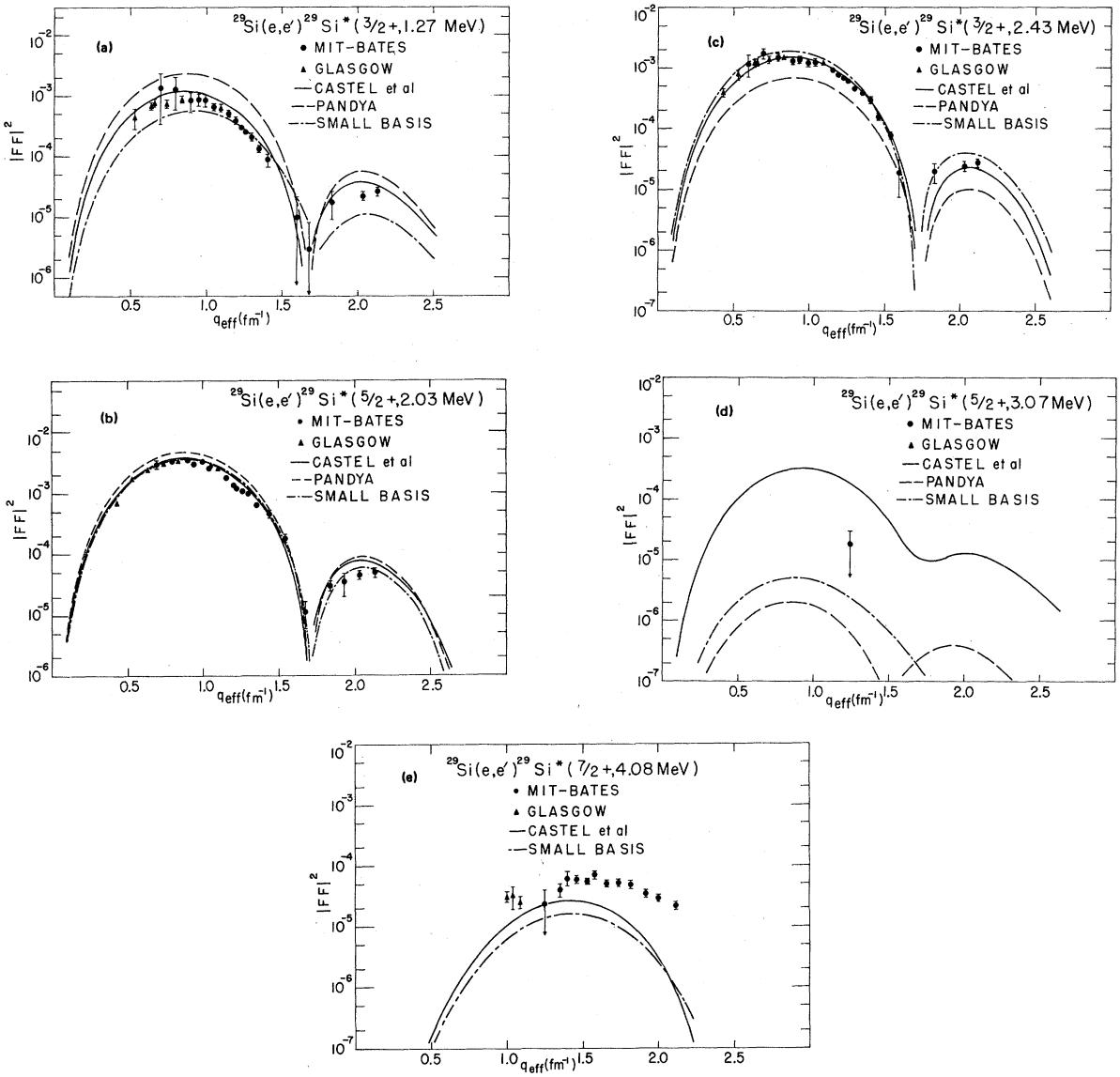

FIG. 5. Squared form factors for electron scattering from the low-lying levels in ^{29}Si. (a) $\frac{3}{2}^+$(1.27 MeV) level. (b) $\frac{5}{2}^+$(2.03 MeV) level. (c) $\frac{3}{2}^+$(2.43 MeV) level. (d) $\frac{5}{2}^+$(3.07 MeV) level. (e) $\frac{7}{2}^+$(4.08 MeV) level. The present data are shown as solid circles and the data of Ref. 17 are shown as solid triangles. Also shown are theoretical curves calculated from the three sets of eigenvectors as described in text.

state and transitions between excited states. Since ground state to one-phonon 2+ and two-phonon 4+ PHRME's could be fit to the data, these PHRME's are more independent of the choice of the model than PHRME's between two excited ^{28}Si states. However, these excited core state PHRME's contribute only a few percent to the form factors of the ^{29}Si states except for the 4.08 MeV level. This level contains sizable PHRME's between excited ^{28}Si levels.

To determine which form factors are most sensitive to the SPRME calculations, Coulomb and transverse electric SPRME's were set equal to zero. When this was done three form factors changed by more than 10%: the 1.27 MeV $\frac{3}{2}$+, 3.07 MeV $\frac{5}{2}$+, and 4.08 MeV $\frac{7}{2}$+ levels. Clearly, these form factors contain significant single-particle transition strengths, and will be influenced by errors in calculating the SPRME's. In fact, as can be seen by inspection of Figs. 5(a)–(e), the calculated form factors of the 1.27 MeV level and especially the 4.08 MeV level do not agree with the experimental data as well as the calculated form factors for the 2.03 and 2.43 MeV levels.

The latter two levels are dominated by the measured core form factors in ^{28}Si, and the fit largely depends on the nature of the coupling and not the details of the SPRME's or the model for the core. On the other hand, the 1.27 and 4.08 MeV levels contain significant strength from SPRME's and/or PHRME's between excited ^{28}Si states and are more sensitive to the details of the core and valence neutron.

V. CONCLUSIONS

Within the framework of the model used, the following conclusions are drawn from these data:

(1) There appears to be very little $1d_{5/2}$ strength in the low-lying levels of ^{29}Si.

(2) The low-lying levels in ^{29}Si can be described as a particle with effective charge $0.5e$ weakly coupled to a ^{28}Si core.

ACKNOWLEDGMENTS

The authors extend their sincere thanks to Dr. Robert Wolfson and Mr. Paul Grubenskas of Varian Vaccum Division, Lexington, Massachusetts, for providing the cleaved blanks for the silicon targets; to Mr. George Sechen for his care and patience in etching the targets to their final thickness; to the Bates Linac Operations Staff for their dedication during the data acquisition; and to Dr. E. Moniz for numerous stimulating discussions. This work was supported by the United States Department of Energy under Contract No. EY-76-C-02-3069.

---

*Present address: Raytheon Company, Missile Systems Division, Bedford, Massachusetts.

†Present address: Department of Physics, University of Virginia, Charlottesville, Virginia.

[1]L. L. Foldy and F. J. Milford, Phys. Rev. 80, 751 (1950).

[2]J. Rainwater, Phys. Rev. 79, 432 (1950).

[3]A. Bohr, K. Dan Vidensk. Selsk. Mat. Fys. Medd. 26, No. 14 (1952).

[4]A. Kerman, Phys. Rev. 92, 1196 (1953).

[5]D. C. Choudhury, K. Dan. Vidensk. Selsk. Mat. Fys. Medd. 28, No. 4 (1954).

[6]F. J. Milford, Phys. Rev. 93, 1297 (1954).

[7]A. Bohr and B. Mottelson, K. Dan Vidensk. Selsk. Mat. Fys. Medd. 27, No. 16 (1953).

[8]S. P. Pandya, Prog. Theor. Phys. 21, 431 (1959).

[9]F. G. Bailey and D. C. Choudhury, Nucl. Phys. A144, 628 (1970).

[10]B. Castel, K. W. C. Stewart, and M. Harvey, Can. J. Phys. 48, 1490 (1970).

[11]H. Liesem, Z. Phys. 196, 174 (1966).

[12]G. A. Savitskii, N. C. Afanosev, I. S. Gul'karov, V. D. Kovalev, A. S. Omelaenko, V. M. Khrastanov, and N. G. Shevchenko Yad. Fiz. 8, 648 (1969) [Sov. J. Nucl. Phys. 8, 376 (1969)].

[13]G. Mulhaupt, Ph.D. thesis, Universität Mainz, 1970 (unpublished).

[14]A. Nakada and Y. Torizuka, J. Phys. Soc. Jpn. 32, 1 (1972).

[15]G. C. Li, I. Sick, and M. R. Yearian, Phys. Rev. C 9, 1861 (1974).

[16]S. W. Brain, A. Johnston, W. A. Gillespie, E. W. Lees, and R. P. Singhal, J. Phys. G 3, 821 (1977).

[17]S. W. Brain, A. Johnston, W. A. Gillespie, E. W. Lees, and R. P. Singhal, J. Phys. G 3, 681 (1977).

[18]W. Bertozzi, J. Haimson, C. P. Sargent, and W. Turchinetz, IEEE Trans. Nucl. Sci., NS-14, 191 (1967).

[19]S. Kowalski, W. Bertozzi, and C. P. Sargent, in *Medium Energy Nuclear Physics with Electron Linear Accelerators*, MIT 1967 Summer Study [U.S. AEC, Div. of Technical Information (TID-24667), 1967], p. 39.

[20]W. Bertozzi, M. V. Hynes, C. P. Sargent, W. Turchinetz, and C. Williamson, Nucl. Instrum. Methods 162, 211 (1979).

[21]W. Bertozzi, M. V. Hynes, C. P. Sargent, C. Creswell, P. C. Dunn, A. Hirsch, M. Leitch, B. Norum, F. N. Rad, and T. Sasanuma, Nucl. Instrum. Methods 141, 457 (1977).

[22]R. Liljestrand, G. Blanpied, G. W. Hoffmann, J. E. Spencer, and J. R. Rhodes, Nucl. Instrum. Methods 138, 471 (1976).

[23]P. R. Bevington, *Data Reduction and Error Analysis for the Physical Sciences* (McGraw-Hill, New York, 1969).

[24]K. E. Whitner, Masters thesis, MIT, 1979 (unpublished).

[25]J. D. Walecka, Phys. Rev. 126, 653 (1962).

[26]R. H. Helm, Phys. Rev. 104, 1466 (1956).

[27]R. S. Willey, Nucl. Phys. 40, 529 (1963).

[28]L. J. Tassie and F. C. Barker, Phys. Rev. 111, 940 (1958).

[29]S. G. Nilsson, K. Dan. Vidensk. Selsk. Mat. Fys. Medd. 29, No. 16 (1955).